Analysis for burst gravitational waves with TAMA300 data

Masaki Ando†, K. Arai‡, R. Takahashi‡, D. Tatsumi‡, P. Beyersdorf‡, S. Kawamura‡, S. Miyoki§, N. Mio‖, S. Moriwaki‖, K. Numata†, N. Kanda¶, Y. Aso†, M.-K. Fujimoto‡, K. Tsubono†, K. Kuroda§, and the TAMA collaboration[+]

† Department of Physics, University of Tokyo, 7-3-1 Hongo, Bunkyo-ku, Tokyo 113-0033, Japan,
‡ Space-Time Astronomy Section, National Astronomical Observatory,
§ Institute for Cosmic Ray Research, University of Tokyo,
‖ Department of Advanced Materials Science, University of Tokyo,
¶ Department of Physics, Osaka City University,
[+] Earthquake Research Institute, University of Tokyo,
Institute for Laser Science, University of Electro-Communications,
High Energy Accelerator Research Organization,
Department of Earth and Space Science, Osaka University,
Yukawa Institute for Theoretical Physics, Kyoto University,
Max-Planck-Institut für Quantenoptik,
National Research Laboratory of Metrology,
Faculty of Science and Technology, Hirosaki University,
Department of Astronomy, University of Tokyo,
Department of Physics, Kinki University,
Department of Materials Science and Engineering, Tokyo Denki University,
Precision Engineering Division, Tokai University,
Astronomical Institute, Tohoku University,
Department of Physics, Niigata University,
Department of Physics, Hiroshima University.

Abstract.

We present the analysis results of the TAMA 1000 hours of data, targeting at short bursts of gravitational waves. In this analysis, we used an excess power filter for the signal detection, and time-scale selection of the event candidates for non-Gaussian noise rejection. As a result, no evidence of the detection was found, and obtained the false alarm rate of 4 events/hour for $h \sim 3 \times 10^{-17}$ gravitational waves. Time dependence analysis of the event candidates show that the false alarms are mainly caused by the non-Gaussian noises originated in the seismic disturbances in daytime. These results show that further improvements in the detector and analysis methods are requires for the signal detection.

PACS numbers: 04.80.Nn

E-mail: ando@granite.phys.s.u-tokyo.ac.jp

1. Introduction

A burst gravitational wave, which is emitted from a stellar-core collapse in a supernova explosion, is one of the targets in interferometric gravitational-wave detectors [1, 2, 3, 4, 5]. For the detection of these signals, several data analysis method called 'burst filters' have been proposed [6, 7, 8, 9] and are applied to the real data from detectors. In the analysis of burst signals, a set of precise waveform templates which covers the source parameters is not available, while some typical waveforms were obtained by numerical simulations [10]. Thus, the burst filters are designed to have high sensitivity to unusual events in the detector outputs, with little assumption on the waveform of the signal. Performances of these filters have been investigated in well-defined statistics with ideal Gaussian, stationary noise.

However, there are several practical problems in the implementation of these filters to the real analysis. Among them, non-Gaussian noises in the detector output affect the analysis results significantly; these noises would be caused by environmental disturbances, instability of the detector, and so on. In the case of an inspiral gravitational-wave search, in which waveforms are well predicted, most of the non-Gaussian noises are rejected by the signal behavior (by the method called χ^2 rejection) [11, 12]. On the other hand, in case of a burst gravitational-wave search, non-Gaussian noises appear as unusual events, causing false alarms in the output of the burst filter. As a result, real signals are likely to be buried in these false alarms, or likely to be dismissed with a larger detection threshold set to reduce false alarms. Thus, rejection of non-Gaussian noises is crucial for effective detection.

In this article, we present the search results of burst gravitational wave signals using data from TAMA300. TAMA300 is a Japanese interferometric gravitational wave detector, located at the Mitaka campus of the national astronomical observatory of Japan (NAOJ) in Tokyo. In this analysis, 1000 hours of data obtained in the 6th data-taking run (DT6) of TAMA300 (in the summer of 2001) were used [13]. We used an excess power filter as a burst filter, and reject the non-Gaussian noises with time-scale selection [14].

2. Burst wave analysis method

In TAMA, the 6th data-taking run (DT6) was carried out in the summer of 2001. It was a 50-day observation run aiming to collect 1000 hours of data. The output of the TAMA300 detector was recorded with a 20 kHz, 16 bit data-acquisition system, and stored in DLT tapes. During the run, a 625 Hz sinusoidal signal was injected to the front mirrors of the detector. Recorded data includes this sinusoidal signal, which enables us to calibrate the detector sensitivity continuously [15]. Using this data, burst gravitational wave analysis was done with the following steps:

(i) Make a spectrogram from the raw data by calculating the noise spectrum for every 200 msec and with an overlap of 175 msec. Spectrograms are calibrated to a unit

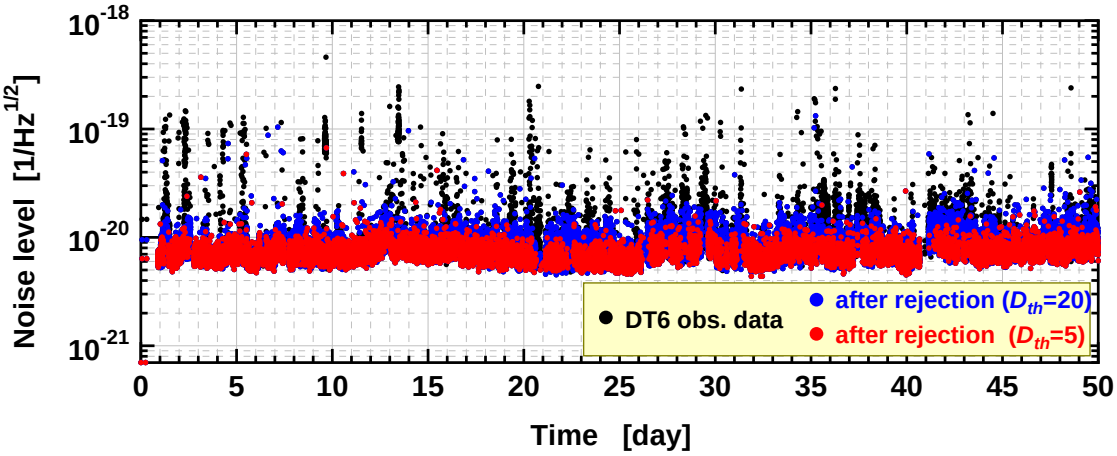

Figure 1. Averaged power in every 3.2 sec in the TAMA data taking 6 (DT6). The black points represent all of the data points in DT6. The gray points are the survived ones after non-Gaussian noise rejection.

of strain. Here, the calibration factor from the voltage to strain, the interferometer response, the effect of a control loop, and the transfer function of the whitening filter are taken into account.

(ii) Sum up the power in selected frequency components in each spectrum. As a result, we obtained time series of noise power in the selected frequency band. The frequency components to be used were selected to avoid the frequency region with large noises, AC line peaks, and violin mode peaks of suspension wires. In this analysis, the selected frequency components were between 400 Hz and 1.3 kHz, and the total frequency band used in the summation of the noise power was about 500 Hz.

(iii) Total power and the second-order component of the noise power were calculated in every 3.2 sec data chunk in order to evaluate the time scale of the non-Gaussian event [14]. The events were evaluated by the 'gravitational-wave likelihood' D based on their time scale; the distribution almost follows $\exp(D^2/2)$ in case of Gaussian noises and typical gravitational waveforms. If D of events were large, meaning that the time scale the events were much longer than that of the real signal, these events were considered to be non-Gaussian noise caused by the detector instability, and data in the corresponding time were treated as dead times of the detector.

(iv) By setting a threshold for the total noise power, event candidate list was made. Continuous cluster of the large power data was considered to be a single event, and peak power and corresponding time were recorded. In this analysis, we mainly used a threshold of $h = 6.6 \times 10^{-20}/\sqrt{\mathrm{Hz}}$, which corresponds to $h = 3 \times 10^{-17}$ in strain for 1 msec short burst signal with 500 Hz analysis bandwidth.

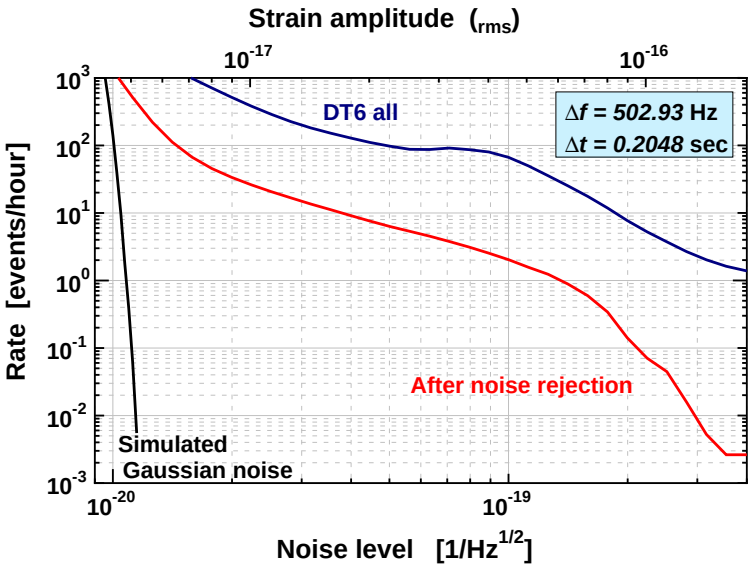

Figure 2. Rate of the events candidates. Larger events than the given noise power level were counted. The analysis results for the original DT6 data, data after non-Gaussian noise rejection, and simulated Gaussian data are shown.

3. Evaluation results

Figure 1 shows the time series of the noise power in DT6 (only one representative points in every continuous 2560 points are plotted in this figure to show the results clearer). The black points represent the data points in observation state in DT6. We can see that the noise power was not so stationary. In particular, they usually became large in the daytime because of larger seismic disturbances. The gray points in Fig. 1 are survived ones after non-Gaussian noise rejection; about 23% and 60% of the data were rejected for the $D_{\rm th} = 20$ and the $D_{\rm th} = 5$ cases, respectively. We see that most of the huge noise points in day time were rejected by this non-Gaussian noise rejection procedure. Here, note that the false dismissal rate by the non-Gaussian noise rejection is less than 1 ppm for $D_{\rm th} = 5$, which was evaluated by a theoretical analysis and a Monte-Carlo simulation with Gaussian noise and typical gravitational wave signal waveforms.

The event-rate curves are shown in Fig. 2; the rate of event candidates with larger noise power than the given value are plotted. Also from this plot, we can see that the event rate was reduced by the non-Gaussian noise rejection. For example, an event rate larger than $3 \times 10^{-19}/\sqrt{\rm Hz}$ was reduced by a factor of 300 to be 10^{-2} events/hour. An event rate larger than $6.6 \times 10^{-20}/\sqrt{\rm Hz}$ was reduced by a factor of 20 to be 4 events/hour; this noise level corresponds to a gravitational-wave amplitude of $h \sim 3 \times 10^{-17}$ in strain for a 1 msec short-burst signal model.

Results for simulated Gaussian noises are also plotted in Fig. 2; the same excess power filter and non-Gaussian noise rejection method as the real data analysis were applied to

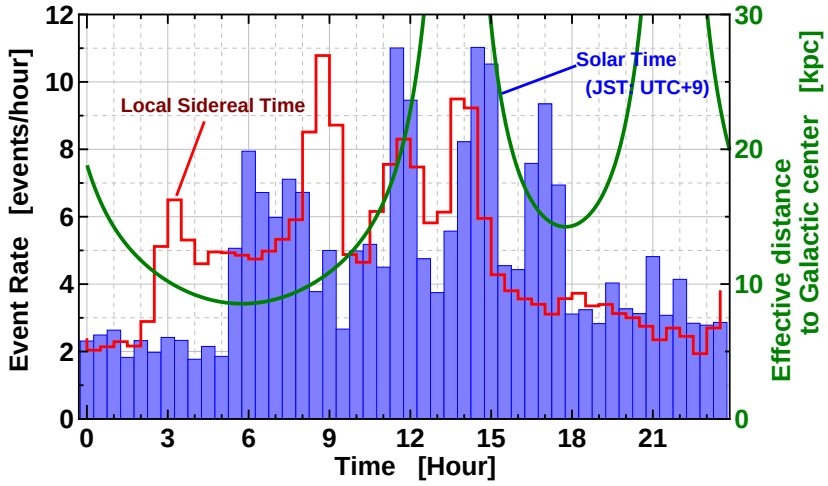

Figure 3. Time dependence of the event candidates. Event candidates with larger power than a threshold of $h = 6.6 \times 10^{-20}/\sqrt{\text{Hz}}$ are counted. Event rate and effective distance to the galactic center for a given local sidereal time are also plotted with staircase and curve plots, respectively.

the Gaussian noises. This show that the results for the DT6 real data is far from the Gaussian noise results, even after non-Gaussian rejection. Since the excess from the Gaussian noise is too huge, it will be natural to consider that this was caused by the non-Gaussian noises in the detector, rather than by gravitational-wave bursts. Thus, further improvement of the detector behavior, better analysis methods, and a coincidence analysis with other detectors are required in order to reduce non-Gaussian noises and see burst gravitational-wave signals.

Figure 3 shows the time dependence of the event rate with a threshold of $h = 6.6 \times 10^{-20}/\sqrt{\text{Hz}}$. Event-rate dependence on the local sidereal time are also plotted in Fig. 3. If the events are originated by the real signal from astronomical sources, there would be a clustering of the events at a certain sidereal time. This is because the detector has better sensitivity to the direction of the galactic center in a certain sidereal time (sidereal time of around 6 in Fig. 3), and not so much in the other sidereal time [20, 21]. As a result, Fig. 3 shows that the event rates become small to about 2 events/hour in midnight, and becomes larger by a factor of 5 in daytime. The results of sidereal time analysis was mostly affected by this daily change, and show little dependence on the position of the galactic center. This results also indicates that the large event rate were caused by detector instability, mostly by seismic disturbance in daytime, rather than the real gravitational-wave signal.

4. Conclusion

We analyzed 1000 hours of data obtained in the 6-th data taking run of TAMA300, targeting at short bursts of gravitational waves. As a result, no evidence of the detection was found, and obtained the event rate (false alarm rate) of 4 events/hour for $h = 3\times10^{-17}$ gravitational waves. The time-dependence analysis of the event candidates show that the false alarms are mainly caused by the non-Gaussian noises originated in the seismic disturbances in daytime, in spite of an effective reduction of non-Gaussian noises in our analysis. Thus, improvement of the detector, better analysis method [19], and a coincidence analysis with the other detectors [16, 17, 18] are required for the reduction of the non-Gaussian noises, and the detection of burst gravitational waves.

Acknowledgments

This research is supported in part by a Grant-in-Aid for Scientific Research on Priority Areas (415) of the Ministry of Education, Culture, Sports, Science and Technology.

References

[1] Abramovici A *et al* 1992 *Science* **256** 325.
[2] The VIRGO collaboration 1997 *VIRGO Final Design Report* VIR-TRE-1000-13.
[3] Danzmann K *et al* 1994 *Proposal for a 600m Laser-Interferometric Gravitational Wave Antenna* (Max-Planck-Institut für Quantenoptik Report) 190.
[4] Tsubono K 1995 *Gravitational Wave Experiments* (edited by E. Coccia, G. Pizzella, and F. Ronga, World Scientific), p. 112-114, Kuroda K *et al* 1997 *Gravitational Waves: Sources and Detectors* (edited by I. Ciufolini and F. Fidecaro, World Scientific), p. 100-107.
[5] Ando M *et al* 2001 *Phys. Rev. Lett.* **86** 3950.
[6] Anderson W G *et al* 2001 *Phys. Rev.* D **63** 042003, Anderson W G *et al* 1999 *Phys. Rev.* D **60** 102001.
[7] Mohanty S D 2000 *Phys. Rev.* D **61** 122002.
[8] Pradier T *et al* 2001 *Phys. Rev.* D **63** 042002, Arnaud N *et al* 2003 *Phys. Rev.* D **67** 062004-1.
[9] Arnaud N *et al* 1999 *Phys. Rev.* D **59** 082002.
[10] Zwerger Z and MÏller 1997 *Astron. Astrophys.* **317** L79, Dimmelmeier H *et al* 2002 *Astron. Astrophys.* **393** 523.
[11] Allen B *et al* 1999 *Phys. Rev. Lett.* **83** 1498.
[12] Tagoshi H *et al* 2001 *Phys. Rev.* D **63** 062001.
[13] M. Ando 2002 *Class. Quantum Grav.* **19** 1409.
[14] M. Ando *et al* 2003 *Class. Quantum Grav.* **20** S697.
[15] N. Kanda and the TAMA Collaboration 2000 Int. J. Mod. Phys. D **9** 233, D. Tatsumi *et al* 2004 in this issue.
[16] Astone P *et al* 1999 *Phys. Rev.* D **59** 122001, Allen Z A *et al* 2000 *Phys. Rev. Lett.* **85** 5046.
[17] Nicholson D *et al* 1996 *Phys. Lett.* A **218** 175.
[18] Astone P *et al* 1994 *Class. Quantum Grav.* **11** 2093.
[19] Creighton J D E 1999 *Phys. Rev.* D **60** 021101, Heng I S *et al* 2002 *Class. Quantum Grav.* **19** 1889.
[20] P. Astone *et al* 2002 *Class. Quantum Grav.* **19** 5449.
[21] G. Paturel, *et al* 2003 ApJ **592** L99.